Fuel 206 (2017) 580–592

Contents lists available at ScienceDirect

Fuel

journal homepage: www.elsevier.com/locate/fuel

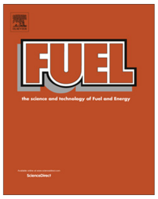

Multi-objective optimization of thermally coupled reactor of CCR naphtha reforming in presence of SO_2 oxidation to boost the gasoline octane number and hydrogen

Reza Saeedi, Davood Iranshahi *

Department of Chemical Engineering, Amirkabir University of Technology (Tehran Polytechnic), No. 424, Hafez Avenue, Tehran 15914, Iran

HIGHLIGHTS

- A novel thermally coupled reactor in CCR naphtha reforming process is modeled.
- Exothermic oxidation of SO_2 to SO_3 was used for coupling purpose.
- A new kinetic model involving 32 pseudo-component and 84 reactions is proposed.
- Multi-objective optimization is carried out to obtain the maximum amount of valuable product.
- Maximizing the octane number and minimizing the light ends are the best possible objective function.

ARTICLE INFO

Article history:
Received 17 December 2016
Received in revised form 22 February 2017
Accepted 4 April 2017

Keywords:
Naphtha reforming
Continuous catalyst regeneration
Thermal coupling
Multi-objective optimization
Gasoline
Octane number

ABSTRACT

In this study, thermal coupling approach was used in catalytic naphtha reforming process with continuous catalyst regeneration with the intention of energy saving and mitigation of environmental issues. Due to the endothermic nature of catalytic naphtha reforming process, exothermic oxidation of SO_2 to SO_3 was used for coupling purpose. The kinetic model used in this study comprises 32 pseudo-components and 84 reactions which represent the main reactions of the process. Due to the several products in this process, multi-objective optimization and three cases are carried out to obtain the maximum amount of valuable products such as aromatics and hydrogen and minimum amount of light ends as well as maximizing the octane number of the exit stream. Maximizing the aromatics (octane number) and minimizing the light ends in reformate are the best possible objective functions in this research. The results of this study can be applied in different situations with regard to the required process goal e.g. maximizing the hydrogen production or research octane number (RON) of the products.

1. Introduction

Fossil fuels, still as the main source of fulfilling human need for energy, are accompanied with sulfur which is categorized as a pollutant agent. This element can be transformed into other sulfurous compounds such as SO_2 and H_2S during fuel combustion or refining processes, respectively. However, these compounds are also not environmentally friendly and can lead to severe human health issues through inhalation or exposure. Therefore, it is of great importance to contemplate beginning a sustainable plan for reducing the side effects of fuels that can result in an environmentally-benign process. Some efforts have been made with the purpose of removal or reducing the destructive effect of SO_2 [1–4]. Among these methods catalytic oxidation of SO_2 to SO_3 has been widely employed [5–7]. The main product, SO_3, can act as a precursor for production of useful substances for instance sulfuric acid, thionyl chloride, ammonium sulfate, etc. This oxidation process can be performed in absence or presence of catalysts such as V_2O_5 [5]. However, the latter is associated with higher rate of reaction. Some valuable studies on this process have been reported in literature. Dunn et al. examined the oxidation process of SO_2 to SO_3 over supported vanadium catalysts [5]. Jorgensen et al. investigated oxidation of SO_2 in the presence of homogeneous and heterogeneous catalysts, experimentally [6].

On the other side, naphtha reforming is one of the main processes performed in refineries with the aim of transforming low-octane naphtha to high-octane reformate, as well as production of aromatics and hydrogen [8]. Three major configurations are typically utilized for carrying out this process: cyclic regenerative

---

* Corresponding author.
E-mail address: iranshahi@aut.ac.ir (D. Iranshahi).

http://dx.doi.org/10.1016/j.fuel.2017.04.024
0016-2361/© 2017 Elsevier Ltd. All rights reserved.

Nomenclature

a_i	catalyst activity in endothermic reaction side
a_A	acidic function activity in endothermic reaction side
a_{C_A}	acidic function activity for coke formation in endothermic reaction side
a_{C_M}	metallic function activity for coke formation in endothermic reaction side
a_M	metallic function activity in endothermic reaction side
A_r	cross section area of reactor in radial direction, m^2
A_p	available side area for heat transfer, m^2
C	concentration in endothermic reaction side, kmol m^{-3}
C^{Exo}	concentration in exothermic reaction side, kmol m^{-3}
C_{ACP}	alkyl-cyclopentane concentration, kmol m^{-3}
C_{C_A}	coke weight fraction on acidic function of catalyst in endothermic reaction side, kg kgcat^{-1}
C_{C_M}	coke weight fraction on metallic function of catalyst in endothermic reaction side, kg kgcat^{-1}
C_p	specific heat capacity at constant pressure in endothermic reaction side, kJ kmol^{-1} K^{-1}
C_P^{Exo}	specific heat capacity at constant pressure in exothermic reaction side, kJ kmol^{-1} K^{-1}
C_v	specific heat capacity at constant volume in endothermic reaction side, kJ kmol^{-1} K^{-1}
C_v^{Exo}	specific heat capacity at constant volume in exothermic reaction side, kJ kmol^{-1} K^{-1}
C_T	total concentration in endothermic reaction side, kmol m^{-3}
C_T^{Exo}	total concentration in exothermic reaction side, kmol m^{-3}
d_p	particle diameter, m
dr	control volume thickness in radial direction, m
dz	control volume length, m
D_e	effective diffusivity, m^2 s^{-1}
E_c	coke formation activation energy in endothermic reaction side, J mol^{-1}
F_j	molar flow rate of component j in endothermic reaction side, kmol h^{-1}
F_j^{Exo}	molar flow rate of component j in exothermic reaction side, kmol h^{-1}
F_T	total molar flow rate in endothermic reaction side, kmol h^{-1}
F_T^{Exo}	total molar flow rate in exothermic reaction side, kmol h^{-1}
F_f	molar flow rate of endothermic side, kmol h^{-1}
H_j	enthalpy of component j in endothermic reaction side, J mol^{-1}
H_j^{Exo}	enthalpy of component j in exothermic reaction side, J mol^{-1}
k	thermal conductivity, W m^{-1} K^{-1}
k_{C_A}	constant of deactivation equation for acidic function in endothermic reaction side, kg kgcat^{-1} kPa$_1^n$ m$^{1.5}$ kmol$^{-1.5}$
k_{C_M}	constant of deactivation equation for metallic function in endothermic reaction side, kg kgcat^{-1} kPa$_1^n$ m$^{1.5}$ kmol$^{-1.5}$
k_{eff}	effective thermal conductivity, W m^{-1} k^{-1}
k_{in}	reaction rate constant for endothermic reaction (in)
K_{in}	equilibrium constant for endothermic reaction (in)
L	length of reactor, m
m	number of reactions in endothermic reaction side
M_j	molecular weight of component j, kg kmol^{-1}
M	mean molecular weight in the flow, kg kmol^{-1}
n	number of components in endothermic reaction side
n_1	constant of deactivation equation in endothermic reaction side
n_2	constant of deactivation equation in endothermic reaction side
n_A	acidic function activity power number in endothermic reaction side
n_{CA}	acidic function activity power number in endothermic reaction side
n_M	metallic function activity power number in endothermic reaction side
n_{C_M}	metallic function activity power number in endothermic reaction side
n'	number of components in exothermic reaction side
N_j	molar flux of component j, kmol m^{-2} h^{-1}
N_t	molar flow rate in exothermic side, kmol h^{-1}
P	total pressure, kPa
P_{A_n}	partial pressure of n carbon aromatic, kPa
P_{ACH_n}	partial pressure of n carbon alkyl-cyclohexane, kPa
P_{ACP_n}	partial pressure of n carbon alkyl-cyclopentane, kPa
P_{H_2}	partial pressure of hydrogen in endothermic reaction side, kPa
P_{H2}	partial pressure of hydrogen in exothermic reaction side, Pa
P_{IP_n}	partial pressure of n carbon iso-paraffin, kPa
P_{NB}	partial pressure of nitrobenzene, Pa
P_{NP_n}	partial pressure of n carbon normal-paraffin, kPa
r	radius, m
r_i	rate of ith reaction, kmol kgcat^{-1} h^{-1}
r_{in}	rate of inth reaction, kmol kgcat^{-1} h^{-1}
r'	rate of hydrogenation of nitrobenzene reaction, mol kgcat^{-1} s^{-1}
r_C^o	rate of coke formation on fresh catalyst in endothermic reaction side, kg kgcat^{-1} h^{-1}
r_{C_A}	rate of coke formation on acidic function of catalyst in endothermic reaction side, kg kgcat^{-1} h^{-1}
r_{C_M}	rate of coke formation on metallic function of catalyst in endothermic reaction side, kg kgcat^{-1} h^{-1}
R	gas constant, J mol^{-1} K^{-1}
R_i	inner diameter, m
R_o	outer diameter, m
$\mathrm{S_a}$	specific surface, m^2 g^{-1}
T	temperature of endothermic reaction side, K
T^{Exo}	temperature of exothermic reaction side, K
U	overall heat transfer coefficient, W m^{-2} K^{-1}
U_j	internal energy of component j, J mol^{-1}
u_r	radial velocity in endothermic reaction side, m s^{-1}
u_r^{Exo}	radial velocity in exothermic reaction side, m s^{-1}
u_z	catalyst axial velocity in endothermic reaction side, m s^{-1}
u_z^{Exo}	catalyst axial velocity in exothermic reaction side, m s^{-1}
y_j	mole fraction of component j

Greek Letters

ε	void fraction of catalyst bed in endothermic reaction side
μ	viscosity, kg m^{-1} s^{-1}
υ_{ij}	stoichiometric coefficient of component j in reaction i in endothermic reaction side
υ_j	stoichiometric coefficient of component j in exothermic reaction side
ρ_b	reactor bulk density in endothermic reaction side, kg m^{-3}
ρ_b^{Exo}	reactor bulk density in exothermic reaction side, kg m^{-3}
ϕ_s	sphericity
θ_1	endothermic reaction side angle
θ_2	exothermic reaction side angle